An Empirical Formula for Resonant Frequency Shift due to Jerusalem-Cross FSS with Substrate on One Side

Hsing-Yi Chen and Shu-Huan Wen

Department of Communications Engineering
Yuan Ze University, Chung-Li, Taoyuan, 32003, Taiwan
eehychen@saturn.yzu.edu.tw, s1058603@mail.yzu.edu.tw

Abstract ─ An empirical formula for calculating the shifted resonant frequencies of Jerusalem-cross frequency selective surfaces (FSSs) with different substrates is derived based on extensive calculations made on widely varying in shifted dual resonant frequencies for substrates with different relative dielectric constants and thickness. The coefficients in the empirical formula were determined by using least-square curve fitting technique to fit 672 sets of shifted resonant frequencies obtained by the HFSS simulator. Numerical results of shifted resonant frequencies obtained from the empirical formula are generally in good agreement with those calculated by the HFSS simulator and measurement. The average error in the shifted resonant frequencies is less than 5 percent. The empirical formula thus provides a simple, inexpensive, and quick method for obtaining optimum geometrical parameters of a dual-band Jerusalem-cross FSS with a substrate consisting of different dielectric constants and thickness for arbitrarily specifying two resonant frequencies.

Index Terms ─ Empirical formula, Jerusalem-cross frequency selective surface, least-square curve fitting, shifted resonant frequencies.

I. INTRODUCTION

Frequency selective surface (FSS) has a wide variety of applications including design of antennas [1-14], realization of polarizers [15], improvement of transmission for signals through energy-saving glass [16-19], synthesis of artificial magnetic conductors (AMCs) and electromagnetic band-gap surfaces (EBGs) [20-23], design of spatial microwave and optical filters [24-36], invention of electromagnetic absorbers [37-42], and creation of planar metamaterials [43]. The FSS is usually formed by periodic arrays of metallic patches or slots of arbitrary geometries. For a patch FSS, it is designed where transmission is minimum but reflection is maximum in the neighborhood of the resonant frequency. Reverse situation happens to the slot FSS. Here transmission is maximum but reflection is minimum in the neighborhood of the resonant frequency.

Three numerical methods are often used to analyze different types of FSS parameters. They are method of moments (MoM) [24], finite-difference time-domain (FDTD) method [44-46], and finite-element method (FEM) [47]. However, these numerical methods can be costly and labor intensive due to the many electromagnetic equations governing FSS theory which should be solved. Alternatively, the equivalent circuit method [48-50] is much simpler than numerical methods for the design of FSS parameters. A limitation of the equivalent circuit method is that it can be used only for a FSS constructed without substrates. It is expected that the presence of the dielectric substrate will shift the resonant frequencies downwards [51-52]. For a Jerusalem-cross FSS with substrate on one side, resonant frequency will be shifted by a factor between unity and $[(\varepsilon_r+1)/2]^{1/2}$ depending on the substrate thickness [25, 53], where ε_r is the relative dielectric constant of the substrate.

Based on equivalent circuit models [49], we proposed the least-square curve fitting technique [54] to quickly obtain optimum values of geometrical parameters of a dual-band Jerusalem-cross FSS without substrate for arbitrarily specifying any dual resonant frequencies [55]. The computational time of the proposed technique is less than 30 seconds for obtaining optimum parameters of a dual-band Jerusalem-cross FSS without substrate. However, the proposed technique has a limitation which is only available for a dual-band Jerusalem-cross FSS without substrate. In order to investigate the shift effect of resonant frequency on a dual-band Jerusalem-cross grid with different substrates, one higher resonant frequency and one lower resonant frequency were first arbitrarily specified. Then optimum geometrical parameters of the dual-band Jerusalem-cross FSS without substrate were quickly obtained by using our proposed technique [55] for the dual resonant frequency response. Based on the same optimum geometrical parameters, the shifted dual resonant frequencies of the Jerusalem-cross grid with different substrates on one side were studied by using the Ansoft high-frequency structure simulator (HFSS, Ansoft, Pittsburgh, PA). After further study on shift effects, we derived an empirical

Submitted On: November 7, 2016
Accepted On: June 13, 2018

formula for quickly obtaining optimum parameters of a dual-band Jerusalem-cross FSS with substrate for arbitrarily specifying any dual resonant frequencies. The empirical formula was derived based on extensive calculations made on widely varying in shifted dual resonant frequencies for substrates with different relative dielectric constants, conductivities, and thickness.

II. JERUSALEM-CROSS FSS WITHOUT SUBSTRATE

Figure 1 shows a Jerusalem-cross FSS without substrate. Its geometrical parameters p, w, s, h, and d are also shown in Fig. 1. Where p is the periodicity of a unit cell, w is the width of the conductive strip, s is the separation distance between adjacent units, h is the width of the end caps of the Jerusalem-cross, and d is the length of the end caps of the Jerusalem-cross. Based on Langley and Drinkwater's studies [49], for any array of thin, continuous, infinitely long, and perfectly conducting Jerusalem-cross FSSs, the Jerusalem-cross FSS can be replaced by an equivalent circuit model. This equivalent circuit can generate one lower resonant frequency f_{0L} (in reflection band), one higher resonant frequency f_{0H} (in reflection band), and a transmission band frequency f_t. For arbitrarily specifying any dual resonant frequencies, the optimum values of geometrical parameters of a dual-band Jerusalem-cross FSS without substrate can be quickly obtained by using our proposed technique [55]. The specified dual resonant frequencies will have a downward trend if the dual-band Jerusalem-cross FSS is constructed with substrate on one side [25], [51-53]. Therefore, it is worth studying further on the down-shifting effect of the dual resonant frequencies on Jerusalem-cross FSS with different substrates.

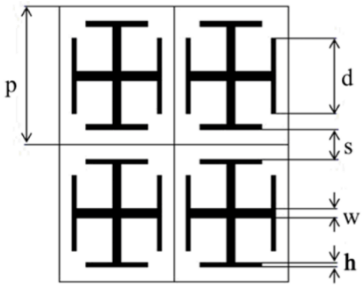

Fig. 1. Geometrical parameters of a FSS constructed with Jerusalem-Cross grids.

III. SUBSTRATE EFFECTS

The FSS is usually printed on a substrate for mechanical strength as shown in Fig. 2. Definitions of geometrical parameters p, w, s, h, and d shown in Fig. 2 are described in Section II. Geometrical parameters t and T are the thickness of the copper foil and the substrate, respectively. Using our proposed technique [55], optimum geometrical parameters (p = 5.33 mm, w = 0.5195 mm, s = 0.3897 mm, h = 0.4311 mm, d = 3.168 mm) of a dual-band Jerusalem-cross FSS without substrate are easily obtained for arbitrarily specifying two resonant frequencies of 16.2 and 50.7 GHz. Based on the same optimum geometrical parameters and assuming t = 0.1 mm and T = 0.0 mm (in air), simulation results of transmission for the Jerusalem-cross FSS without substrate obtained by using the HFSS simulator are shown in Fig. 3. In the simulation, the relative dielectric constant ε_r = 1.0 and conductivity $\sigma = 5.8\times10^7$ S/m of the copper foil were adopted. Obviously, the dual resonant frequencies f_{0L} and f_{0H} are found at 16.2 and 50.7 GHz, respectively. In the following studies, the optimum geometrical parameters (p = 5.33 mm, w = 0.5195 mm, s = 0.3897 mm, h = 0.4311 mm, d = 3.168 mm) and the thickness of copper foil t = 0.1 mm of the dual-band Jerusalem-cross FSS with substrate are always kept unchanged. However, one of the parameters T (thickness of the substrate), ε_r (relative dielectric constant of the substrate), and σ (conductivity of the substrate) is changed in each study. Figure 4 shows the comparison of frequency responses of transmission for the Jerusalem-cross FSS with and without substrate. In HFSS simulations, the relative dielectric constant of the substrate is changed from ε_r = 1.0 to ε_r = 10.0. The thickness and the conductivity of the substrate T = 0.8 mm and $\sigma = 1.3\times10^{-3}$ S/m are kept unchanged, respectively. The relative dielectric constant ε_r = 1.0 means that the substrate is replaced by air. As shown in Fig. 4, the higher resonant frequency f_H decreases from 50 .7 GHz to 23.6 GHz and the lower resonant frequency f_L decreases from 16.2 GHz to 7.5 GHz when the relative dielectric constant increases from ε_r = 1.0 to ε_r = 10.0, respectively. Figure 5 also shows the comparison of frequency responses for transmission of the Jerusalem-cross FSS with and without substrate. In Fig. 5, the thickness of the substrate is changed from T= 0.0 mm to 3.0 mm. The relative dielectric constant and the conductivity of the substrate ε_r = 3.0 and $\sigma = 1.3\times10^{-3}$ S/m are kept unchanged, respectively. The thickness of the substrate T = 0.0 mm also means that the substrate is replaced by air. Figure 5 shows that the higher resonant frequency f_H decreases from 50 .7 GHz to 34.6 GHz and the lower resonant frequency f_L decreases from 16.2 GHz to 11.5 GHz when the thickness of the substrate is changed from T = 0.0 mm to 3.0 mm, respectively. From the resonant frequency responses shown in Fig. 5, it is found that the shift of resonant frequency is a function of the substrate thickness. In terms of resonant wavelength, the variation of the thickness of the substrate is in the range of 0 - 0.2704 λ_{0H} and 0 - 0.0864 λ_{0L}, where λ_{0H} and λ_{0L} are the higher and the lower resonant wavelengths of the FSS without substrate, respectively. The shifting factors of the higher and the lower resonant frequencies are found to be 1.0 - 0.682 and 1.0 - 0.709 for the thickness of the substrate

ranging from 0.0 to 0.2704 λ_{0H} and from 0.0 to 0.0864 λ_{0L}, respectively. Figure 6 shows the frequency response of transmission for the Jerusalem-cross FSS with substrate. In Fig. 6, the conductivity of the substrate is changed from $\sigma = 1.0 \times 10^{-5}$ to 1.0×10^{-1} S/m. The relative dielectric constant $\varepsilon_r = 3.0$ and the thickness of the substrate T = 0.8 mm are kept unchanged. In Fig. 6, it is found that the shift of resonant frequency resulting from the variation of the conductivity of the substrate is insignificant.

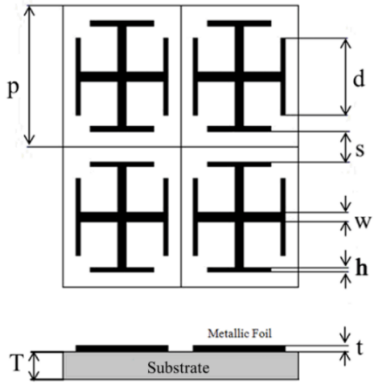

Fig. 2. A Jerusalem-cross FSS with a supporting substrate.

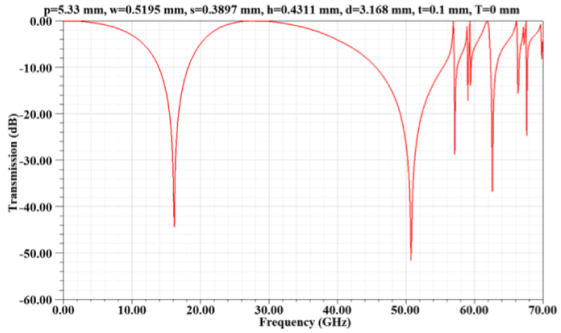

Fig. 3. The frequency responses of transmission of the Jerusalem-cross FSS without substrate.

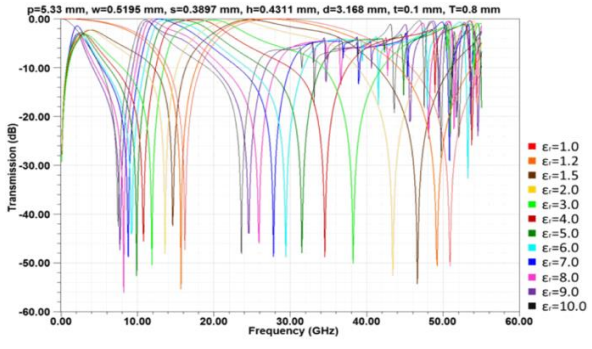

Fig. 4. Comparison of frequency responses of transmission for the Jerusalem-cross FSS with and without substrate. The thickness and the conductivity of the substrate T = 0.8 mm and $\sigma = 1.3 \times 10^{-3}$ S/m are kept unchanged, respectively.

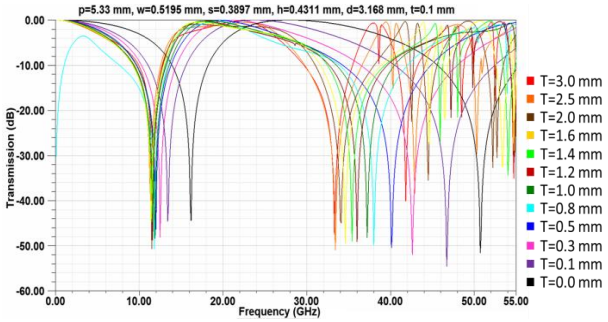

Fig. 5. Comparison of frequency responses of transmission for the Jerusalem-cross FSS with and without substrate. The relative dielectric constant and the conductivity of the substrate $\varepsilon_r = 3.0$ and $\sigma = 1.3 \times 10^{-3}$ S/m are kept unchanged, respectively.

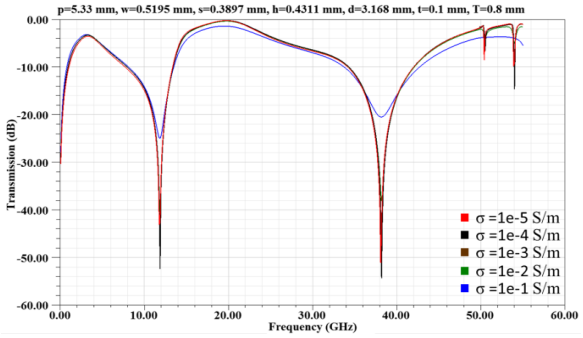

Fig. 6. Frequency responses of transmission for the Jerusalem-cross FSS with substrate. The relative dielectric constant and the thickness of the substrate $\varepsilon_r = 3.0$ and T = 0.8 mm are kept unchanged, respectively.

IV. LEAST-SQUARE CURVE FITTING TECHNIQUE

Figure 7 and Fig. 8 show that the resonant frequencies of a Jerusalem-cross FSS with a substrate are shifted downwards due to increases in the relative dielectric constant of the substrate from 1.0 to 10 and to increases in the thickness of the substrate from 0.0 to 3.0 mm. Based on observation from Figs. 7 and 8, the following empirical formula (1) is proposed to calculate the dual-band resonant frequencies for a Jerusalem-cross FSS with different substrates:

$$f = \frac{A_5 f_0}{(\varepsilon_r + A_1)^{A_2} \times (\mathrm{T} + A_3)^{A_4}}, \qquad (1)$$

where f denotes the higher resonant frequency f_H or the lower resonant frequency f_L of a Jerusalem-cross FSS with different substrates. f_0 denotes the higher resonant frequency f_{0H} or the lower resonant frequency f_{0L} of a Jerusalem-cross FSS without substrate. ε_r and T (mm) are the relative dielectric constant and thickness of the substrate, respectively. A_1, A_2, A_3, A_4, and A_5 are unknown coefficients to be solved for the empirical formula.

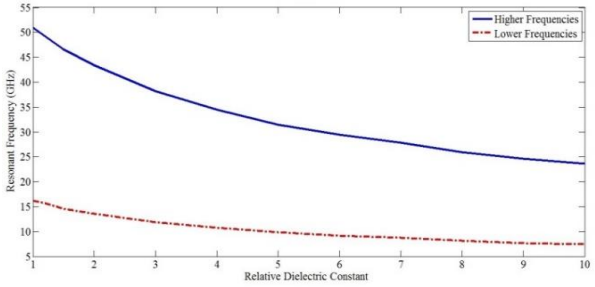

Fig. 7. Resonant frequencies of a Jerusalem-cross FSS with a substrate are shifted downwards due to increases in the relative dielectric constant of the substrate from 1.0 to 10. The thickness and the conductivity of the substrate are T = 0.8 mm and $\sigma = 1.3\times10^{-3}$ S/m, respectively. The geometrical parameters of the FSS are p = 5.33 mm, w = 0.5195 mm, s = 0.3897 mm, h = 0.4311 mm, d = 3.168 mm, respectively.

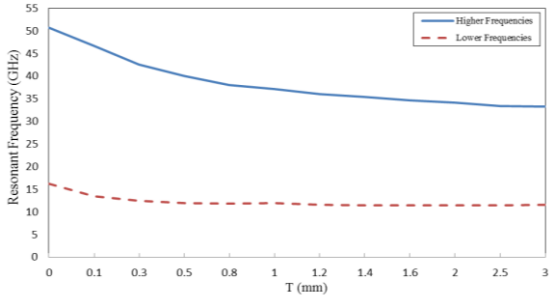

Fig. 8. Resonant frequencies of a Jerusalem-cross FSS with a substrate are shifted downwards due to increases in the thickness of the substrate from 0.0 to 3.0 mm. The relative dielectric constant and the conductivity of the substrate are $\varepsilon_r = 3.0$ and $\sigma = 1.3\times10^{-3}$ S/m, respectively. The geometrical parameters of the FSS are p = 5.33 mm, w = 0.5195 mm, s = 0.3897 mm, h = 0.4311 mm, d = 3.168 mm, respectively.

Basically, the resonant frequency f is a nonlinear function expressed by (1) in terms of the relative dielectric constant ε_r and thickness of the substrate T. The method of differential corrections, together with Newton's iterative method [54], can be used to fit the nonlinear function f. The differential corrections method approximates the nonlinear functions with a linear form that is more convenient to use for an iterative solution. By estimating approximate values of the unknown coefficients $A_1^{(0)}$, $A_2^{(0)}$, $A_3^{(0)}$, $A_4^{(0)}$, and $A_5^{(0)}$, and expanding (1) in a Taylor's series with only the first-order terms retained, we obtain:

$$f = f^{(0)} + \Delta A_1(\frac{\partial f}{\partial A_1})^{(0)} + \Delta A_2(\frac{\partial f}{\partial A_2})^{(0)} + \Delta A_3(\frac{\partial f}{\partial A_3})^{(0)} + \Delta A_4(\frac{\partial f}{\partial A_4})^{(0)} + \Delta A_5(\frac{\partial f}{\partial A_5})^{(0)}. \quad (2)$$

The superscript (0) is used to indicate values obtained after substituting the first guess ($A_1^{(0)}$, $A_2^{(0)}$, $A_3^{(0)}$, $A_4^{(0)}$, and $A_5^{(0)}$), for the unknown coefficients in (1). Equation (2) is a linear function of the correction terms ΔA_1, ΔA_2, ΔA_3, ΔA_4, and ΔA_5, and hence the least-square curve fitting method can be used directly to determine these correction terms. The correction terms, when added to the first guess, give an improved approximation of the unknown coefficients, i.e., $A_1^{(1)} = A_1^{(0)} + \Delta A_1$, $A_2^{(1)} = A_2^{(0)} + \Delta A_2$, $A_3^{(1)} = A_3^{(0)} + \Delta A_3$, $A_5^{(0)}$, and $A_5^{(1)} = A_5^{(0)} + \Delta A_5$. When the improved estimates $A_1^{(1)}$, $A_2^{(1)}$, $A_3^{(1)}$, $A_4^{(1)}$, and $A_5^{(1)}$ are subsequently substituted as new estimates of the unknown coefficients, the Taylor's series reduces to:

$$f = f^{(1)} + \Delta A_1(\frac{\partial f}{\partial A_1})^{(1)} + \Delta A_2(\frac{\partial f}{\partial A_2})^{(1)} + \Delta A_3(\frac{\partial f}{\partial A_3})^{(1)} + \Delta A_4(\frac{\partial f}{\partial A_4})^{(1)} + \Delta A_5(\frac{\partial f}{\partial A_5})^{(1)}, \quad (3)$$

where $f^{(1)}$ as well as its derivatives are obtained by substituting the values of $A_1^{(1)}$, $A_2^{(1)}$, $A_3^{(1)}$, $A_4^{(1)}$, and $A_5^{(1)}$ in (1), respectively. Again, the correction terms ΔA_1, ΔA_2, ΔA_3, ΔA_4, and ΔA_5 are determined using the least-square curve fitting method. The procedure is continued until the solution converges to within a specified accuracy.

The criterion of best fit of the technique of least-square curve fitting is that the sum of the squares of the errors be a minimum expressed by:

$$S = \sum_{i=1}^{N} \varepsilon_i^2 = \text{minimum}, \quad (4)$$

where the term errors ε_i^2 means the difference between the measured (observed) values of the resonant frequencies $f_M(i)$ and computed values from (3) for the i^{th} case, respectively. N is the total number of cases. Substituting (3) into (4), the result yields:

$$S = \sum_{i=1}^{N} [f_M(i) - f(i)]^2. \quad (5)$$

A necessary condition that a minimum for the error function S exists is that the partial derivatives with respect to each of the correction terms ΔA_1, ΔA_2, ΔA_3, ΔA_4, and ΔA_5 be zero. For example, in the first iteration,

$$\frac{\partial S}{\partial(\Delta A_j)} = -2\sum_{i=1}^{N}(\frac{\partial f}{\partial A_j})^{(0)}[f_M(i) - f_1^{(0)} - \Delta A_1(\frac{\partial f}{\partial A_1})^{(0)} - \Delta A_2(\frac{\partial f}{\partial A_2})^{(0)} - \Delta A_3(\frac{\partial f}{\partial A_3})^{(0)} - \Delta A_4(\frac{\partial f}{\partial A_4})^{(0)} - \Delta A_5(\frac{\partial f}{\partial A_5})^{(0)}] = 0, \quad (6)$$

where j= 1, 2, 3, 4, and 5. Equation (6) can be expressed as a matrix equation:

$$\begin{bmatrix} \sum_{i=1}^{N}[(\frac{\partial f}{\partial A_1})^{(0)}]^2 & \cdots & \sum_{i=1}^{N}(\frac{\partial f}{\partial A_1})^{(0)}(\frac{\partial f}{\partial A_5})^{(0)} \\ \sum_{i=1}^{N}(\frac{\partial f}{\partial A_2})^{(0)}(\frac{\partial f}{\partial A_1})^{(0)} & \cdots & \sum_{i=1}^{N}(\frac{\partial f}{\partial A_2})^{(0)}(\frac{\partial f}{\partial A_5})^{(0)} \\ \vdots & & \vdots \\ \sum_{i=1}^{N}(\frac{\partial f}{\partial A_5})^{(0)}(\frac{\partial f}{\partial A_1})^{(0)} & \cdots & \sum_{i=1}^{N}[(\frac{\partial f}{\partial A_5})^{(0)}]^2 \end{bmatrix} \times \begin{bmatrix} \Delta A_1 \\ \Delta A_2 \\ \Delta A_3 \\ \Delta A_4 \\ \Delta A_5 \end{bmatrix} = \begin{bmatrix} \sum_{i=1}^{N}(\frac{\partial f}{\partial A_1})^{(0)}[f_M(i) - f^{(0)}] \\ \sum_{i=1}^{N}(\frac{\partial f}{\partial A_2})^{(0)}[f_M(i) - f^{(0)}] \\ \sum_{i=1}^{N}(\frac{\partial f}{\partial A_3})^{(0)}[f_M(i) - f^{(0)}] \\ \sum_{i=1}^{N}(\frac{\partial f}{\partial A_4})^{(0)}[f_M(i) - f^{(0)}] \\ \sum_{i=1}^{N}(\frac{\partial f}{\partial A_5})^{(0)}[f_M(i) - f^{(0)}] \end{bmatrix}. \quad (7)$$

One can easily solve for the correction terms ΔA_1, ΔA_2, ΔA_3, ΔA_4, and ΔA_5 in (7) by Gaussian elimination method.

V. VALIDATION OF THE EMPIRICAL FORMULA

After curve-fitting 672 sets of shifted resonant frequencies calculated by the HFSS simulator, the coefficients $A_1 = 3.009$, $A_2 = 0.55$, $A_3 = 10.185$ (mm), $A_4 = 0.249$, and $A_5 = 3.66$ are obtained by the least-square curve fitting technique. In order to validate the empirical formula, we compared the shifted resonant frequencies calculated by the HFSS simulator with those obtained by the empirical formula for four different dual-band Jerusalem-cross FSSs with a substrate on one side. Comparisons of shifted resonant frequencies calculated by the HFSS simulator and the empirical formula are shown in Figs. 9-20. From Figs. 9-20, it is shown that numerical results of shifted resonant frequencies obtained from the empirical formula are generally in good agreement with those calculated by the HFSS simulator. The average error in the shifted resonant frequencies is less than 5 percent.

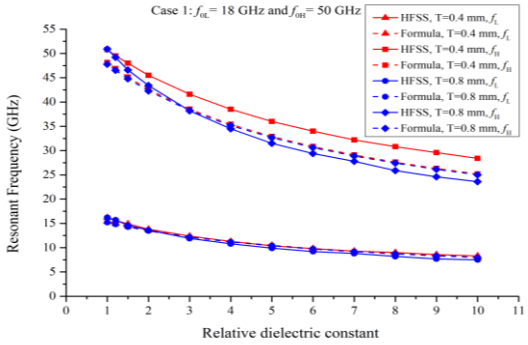

Fig. 9. Comparisons of shifted resonant frequencies calculated by the HFSS simulator and the empirical formula for case 1. The conductivity of the substrate is $\sigma = 1.3 \times 10^{-3}$ S/m (p = 5.33, w = 0.5195, s = 0.3897, h = 0.4311, d = 3.168, and t = 0.1. Unit: mm).

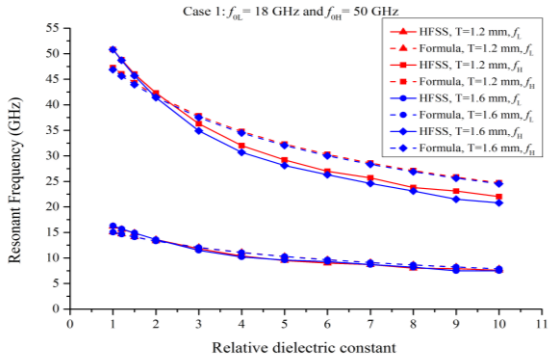

Fig. 10. Comparisons of shifted resonant frequencies calculated by the HFSS simulator and the empirical formula for case 1. The conductivity of the substrate is $\sigma = 1.3 \times 10^{-3}$ S/m (p = 5.33, w = 0.5195, s = 0.3897, h = 0.4311, d = 3.168, and t = 0.1. Unit: mm).

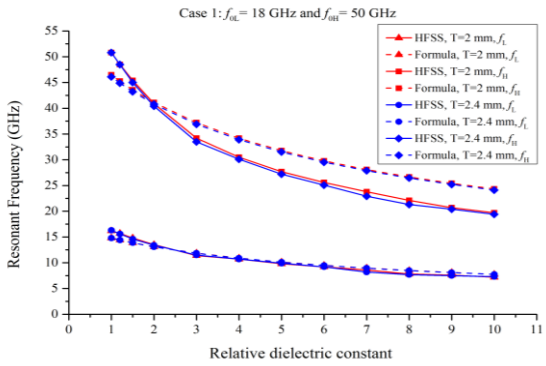

Fig. 11. Comparisons of shifted resonant frequencies calculated by the HFSS simulator and the empirical formula for case 1. The conductivity of the substrate is $\sigma = 1.3 \times 10^{-3}$ S/m (p = 5.33, w = 0.5195, s = 0.3897, h = 0.4311, d = 3.168, and t = 0.1. Unit: mm).

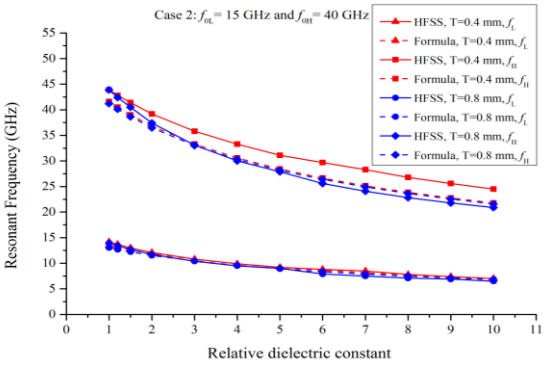

Fig. 12. Comparisons of shifted resonant frequencies calculated by the HFSS simulator and the empirical formula for case 2. The conductivity of the substrate is $\sigma = 1.3 \times 10^{-3}$ S/m.(p = 5.701, w = 0.5038, s = 0.5413, h = 0.4483, d = 3.895, and t = 0.1. Unit: mm).

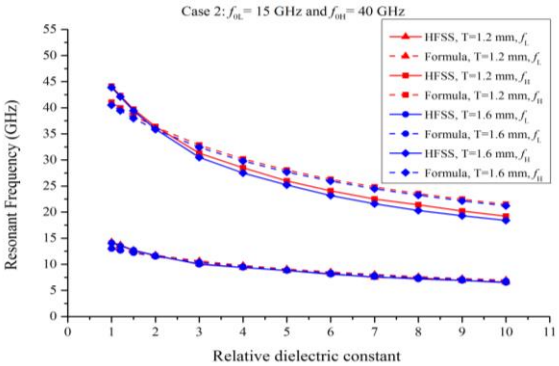

Fig. 13. Comparisons of shifted resonant frequencies calculated by the HFSS simulator and the empirical formula for case 2. The conductivity of the substrate is $\sigma = 1.3 \times 10^{-3}$ S/m (p = 5.701, w = 0.5038, s = 0.5413, h = 0.4483, d = 3.895, and t = 0.1. Unit: mm).

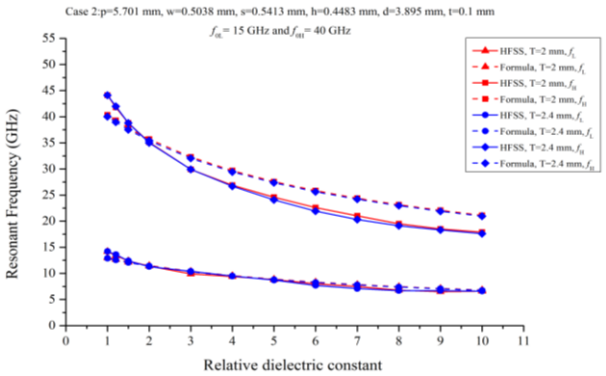

Fig. 14. Comparisons of shifted resonant frequencies calculated by the HFSS simulator and the empirical formula for case 2. The conductivity of the substrate is $\sigma = 1.3 \times 10^{-3}$S/m (p = 5.701, w = 0.5038, s = 0.5413, h = 0.4483, d = 3.895, and t = 0.1. Unit: mm).

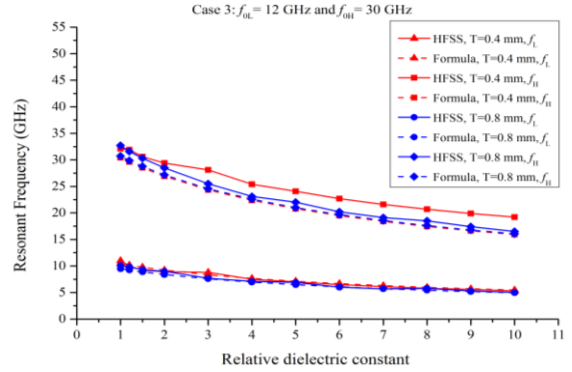

Fig. 15. Comparisons of shifted resonant frequencies calculated by the HFSS simulator and the empirical formula for case 3. The conductivity of the substrate is $\sigma = 1.3 \times 10^{-3}$ S/m.(p = 7.265, w = 0.7234, s = 0.7829, h = 0.5545, d = 5.276, and t = 0.1. Unit: mm).

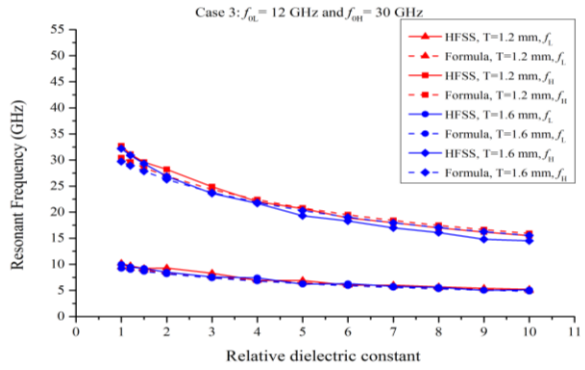

Fig. 16. Comparisons of shifted resonant frequencies calculated by the HFSS simulator and the empirical formula for case 3. The conductivity of the substrate is $\sigma = 1.3 \times 10^{-3}$ S/m (p = 7.265, w = 0.7234, s = 0.7829, h = 0.5545, d = 5.276, and t = 0.1. \ Unit: mm).

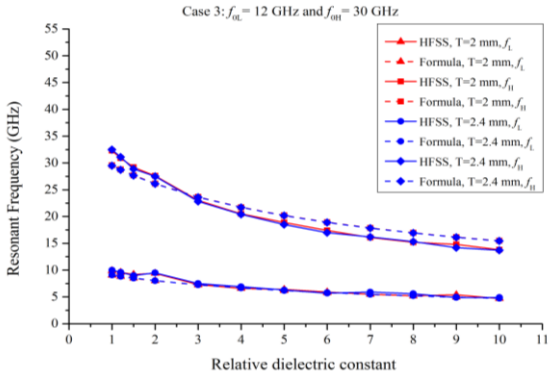

Fig. 17. Comparisons of shifted resonant frequencies calculated by the HFSS simulator and the empirical formula for case 3. The conductivity of the substrate is $\sigma = 1.3 \times 10^{-3}$ S/m (p = 7.265, w = 0.7234, s = 0.7829, h = 0.5545, d = 5.276, and t = 0.1. Unit: mm).

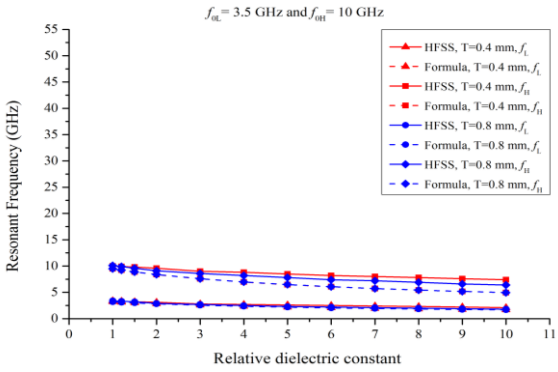

Fig. 18. Comparisons of shifted resonant frequencies calculated by the HFSS simulator and the empirical formula for case 4. The conductivity of the substrate is $\sigma = 1.3 \times 10^{-3}$ S/m (p = 22.77, w = 2.212, s = 1.414, h = 1.524, d = 16.4, and t = 0.1. Unit: mm).

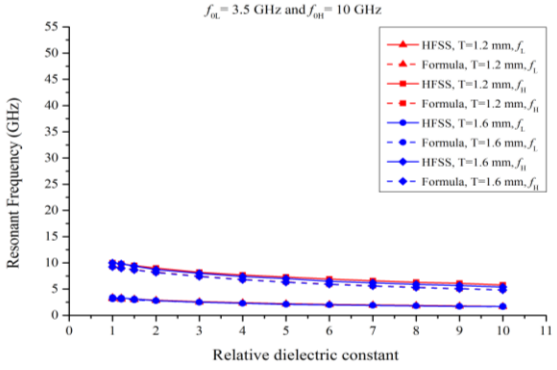

Fig. 19. Comparisons of shifted resonant frequencies calculated by the HFSS simulator and the empirical formula for case 4. The conductivity of the substrate is $\sigma = 1.3 \times 10^{-3}$ S/m (p = 22.77, w = 2.212, s = 1.414, h = 1.524, d = 16.4, and t = 0.1. Unit: mm).

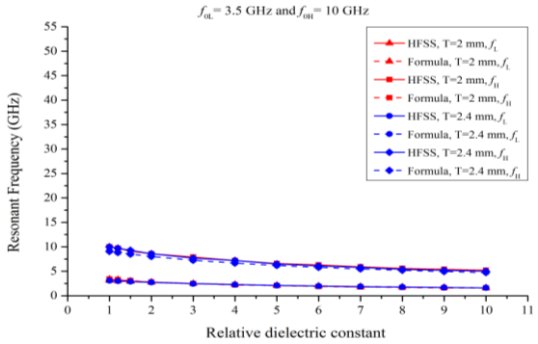

Fig. 20. Comparisons of shifted resonant frequencies calculated by the HFSS simulator and the empirical formula for case 4. The conductivity of the substrate is $\sigma = 1.3 \times 10^{-3}$ S/m (p = 22.77, w = 2.212, s = 1.414, h = 1.524, d = 16.4, and t = 0.1. Unit: mm).

Optimum geometrical parameters of a dual-band Jerusalem-cross FSS with a substrate at arbitrarily specifying two resonant frequencies can be easily and quickly obtained. With Rogers RO4003 substrate as an example, the relative dielectric constant is ε_r = 3.31, dielectric loss tangent = 0.0027, and thickness of substrate is T = 0.8 mm. The dual operating frequencies are arbitrarily given at f_1 = 5.8 GHz and f_2 = 24.0 GHz. The lower resonant frequency f_{0L} = 8.1 GHz and the higher resonant frequency f_{0H} = 33.5 GHz are directly calculated by putting the two specific frequencies of f_1 and f_2, relative dielectric constant, and thickness of substrate in the empirical formula (1), respectively. It takes 20.66 seconds to obtain the optimum geometrical parameters of the dual-band Jerusalem-cross FSS without substrates at the operating frequencies f_{0L} = 8.1 GHz and f_{0H} = 33.5 GHz by the technique presented in [55]. The obtained optimum geometrical parameters are p = 7.577 mm, w = 0.6059 mm, s = 0.1294 mm, h = 0.3793 mm, and d = 4.931 mm. The resonant frequencies of this dual-band Jerusalem-cross FSS without substrate obtained by the HFSS simulator are founded to be f_{0L} = 8.1 GHz and f_{0H} = 31.1 GHz as shown in Fig. 21. There are 0% and 7.1% differences in the lower and higher resonant frequencies calculated by the HFSS simulator and the technique presented in [55], respectively.

The optimum geometrical parameters of the dual-band Jerusalem-cross FSS with substrates at operating frequencies of f_1 and f_2 will be the same as those obtained for the dual-band Jerusalem-cross FSS without substrates at operating frequencies of f_{0L} = 8.1 GHz and f_{0H} = 31.1 GHz. The frequency response of this dual-band Jerusalem-cross FSS with substrate calculated by the HFSS simulator is shown in Fig. 21. The optimum geometrical parameters of the dual-band Jerusalem-cross FSS with substrates are p = 7.577 mm, w = 0.6059 mm, s = 0.1294 mm, h = 0.3793 mm, d = 4.931 mm, t = 0.035 mm, and T = 0.8 mm. From Fig. 21, the dual resonant frequencies of this dual-band Jerusalem-cross FSS with substrate are found to be f_L =5.6 GHz and f_H = 23.3 GHz, respectively. Compared with the arbitrarily given frequencies f_1 = 5.8 GHz and f_2 = 24.0 GHz, there are 3.4% and 2.9% differences in the lower and higher resonant frequencies, respectively. In order to compare with simulation results, the prototype of this dual-band Jerusalem-cross FSS with substrate is fabricated as shown in Fig. 22 and measurements are conducted. Measurement setup is shown in Fig. 23. Comparison of frequency response of this FSS with substrate between simulation results and measurement data is also made as shown in Fig. 21. Good agreement between the simulation results and measurement data has been shown in Fig. 21. From measurement data shown in Fig. 21, it is clear that the lower and higher resonant frequencies are found to be f_L = 5.9 GHz and f_H = 23.4 GHz, respectively.Compared with the arbitrarily given frequencies f_1 = 5.8 GHz and f_2 = 24.0 GHz, there are 1.7% and 2.5% differences in the lower and higher resonant frequencies, respectively.

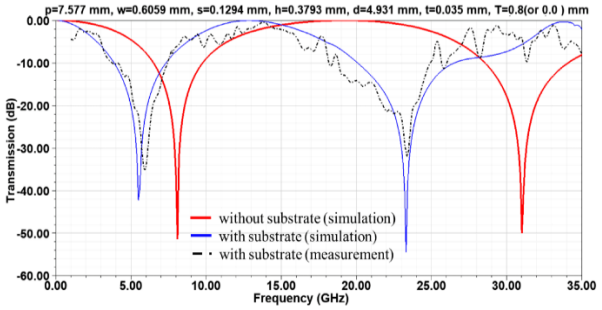

Fig. 21. Frequency responses of a dual-band Jerusalem-cross FSS with and without substrate obtained by HFSS simulator. The geometrical parameters of the FSS are p = 7.577, w = 0.6059, s = 0.1294, h = 0.3793, d = 4.931, t = 0.035, and T = 0.8(or 0.0). Unit: mm.

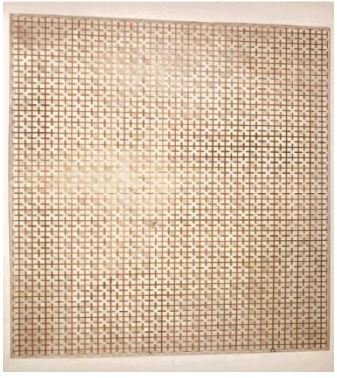

Fig. 22. The prototype of the dual-band Jerusalem-cross FSS with substrate. The geometrical parameters of the FSS are p = 7.577, w = 0.6059, s = 0.1294, h = 0.3793, d = 4.931, t = 0.035, and T = 0.8. Unit: mm.

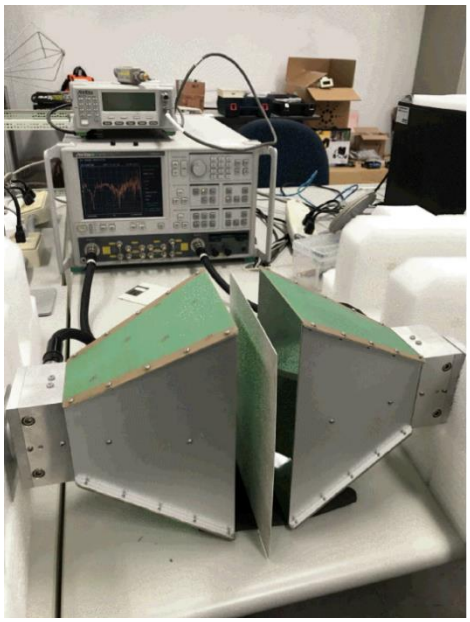

Fig. 23. Measurement setup.

VI. CONCLUSIONS

Based on equivalent circuit models, we proposed a technique to quickly obtain optimum geometrical parameters of a dual-band Jerusalem-cross FSS without substrate for arbitrarily specifying any dual resonant frequencies in the Applied Computational Electromagnetics Society Journal in June, 2015. The drawback of this proposed technique is that it is only available for a dual-band Jerusalem-cross FSS without substrate. In order to overcome the drawback of the proposed technique, firstly, the shifted effects of dual resonant frequencies of Jerusalem-cross FSS with different substrates on one side were extensively studied. After curve-fitting 672 sets of shifted resonant frequencies calculated by the HFSS simulator, we derived an empirical formula for calculating the optimum geometrical parameters of a dual-band Jerusalem-cross FSS with a substrate at arbitrarily specifying two resonant frequencies. The empirical formula is in terms of relative dielectric constant and thickness of substrate. It takes a few seconds to obtain the optimum geometrical parameters of a dual-band Jerusalem-cross FSS with substrates by applying the empirical formula combined with our previous technique. The validity of this empirical formula is checked by comparing simulation results and measurement data of frequency response. The accuracy of the empirical formula is better than 5%. The empirical formula provides a very simple, inexpensive, and quick method for obtaining optimum geometrical parameters of a dual-band Jerusalem-cross FSS with substrate for arbitrarily specifying any dual resonant frequencies. The accuracy of this empirical formula may be within a reasonable error of 5% for substrates with relative dielectric constants in the range from 1.0 to 10, thickness in the range from 0.0 to 3.0 mm, conductivities in the range from 1.0×10^{-5} to 1.0×10^{-1} S/m, and operating frequencies below 50 GHz.

REFERENCES

[1] B. A. Munk, R. J. Luebbers, and R. D. Fulton, "Transmission through a 2-layer array of loaded slots," *IEEE Trans. Antennas Propagat.*, vol. AP22, no. 6, pp. 804-809, Nov. 1974.

[2] M. A. Hiranandani, A. B. Yakovlev, and A. A. Kishk, "Artificial magnetic conductors realized by frequency-selective surfaces on a grounded dielectric slab for antenna applications," *IEE Pro.-Microw. Antennas Propagat.*, vol. 153, no. 5, pp. 487-493, Oct. 2006.

[3] F. Yang and Y. Rahmat-Samii, "Reflection phase characterizations of the EBG ground plane for low profile wire antenna applications," *IEEE Trans. Antennas Propagat*., vol. 51, no. 10, pp. 2691-2703, Oct. 2003.

[4] J. Liang and H. Y. David Yang, "Radiation characteristics of a microstrip patch over an electromagnetic bandgap surface," *IEEE Trans. Antennas Propagat*., vol. 55, no. 6, pp. 1691-1697, June 2007.

[5] D. Sievenpiper, L. Zhang, R. F. Jimenez Broas, N. G. Alex´opolous, and E. Yablonovitch, "High-impedance electromagnetic surfaces with a forbidden frequency band," *IEEE Trans. Microwave Theory Tech.*, vol. 47, no. 11, pp. 2059-2074, Nov. 1999.

[6] Y. Zhang, J. von Hagen, M. Younis, C. Fischer, and W. Wiesbeck, "Planar artificial magnetic conductors and patch antennas," *IEEE Trans. Antennas Propagat.*, vol. 51, no. 10, pp. 2704-2712, Oct. 2003.

[7] X. L. Bao, G. Ruvio, M. J. Ammann, and M. John, "A novel GPS patch antenna on a fractal hi-impedance surface substrate," *IEEE Antennas Wireless Propagat. Lett.*, vol. 5, pp. 323-326, 2006.

[8] H. Mosallaei and K. Sarabandi, "Antenna miniaturization and bandwidth enhancement using a reactive impedance substrate," *IEEE Trans. Antennas Propagat.*, vol. 52, no. 9, pp. 2403-2414, Sep. 2004.

[9] R. F. J. Broas, D. F. Sievenpiper, and E. Yablonovitch, "A high-impedance ground plane applied to a cellphone handset geometry," *IEEE Trans. Microw. Theory Tech.*, vol. 49, no. 7, pp. 1262-1265, July 2001.

[10] A. P. Feresidis, G. Goussetis, S. Wang, and J. C. Vardaxoglou, "Artificial magnetic conductor surfaces and their application to low-profile high-gain planar antennas," *IEEE Trans. Antennas Propagat.*, vol. 53, no. 1, pp. 209-215, Jan. 2005.

[11] H. Li, S. Khan, J. Liu, and S. He, "Parametric

analysis of Sierpinski-like fractal patch antenna for compact and dual band WLAN applications," *Microw. Opt. Technol. Lett.*, vol. 51, no. 1, pp. 36-40, Jan. 2009.

[12] M. Hosseini and S. Bashir, "A novel circularly polarized antenna based on an artificial ground plane," *Progress Electromagn. Research Lett.*, vol. 5, pp. 13-22, 2008.

[13] H.Y. Chen and Y. Tao, "Bandwidth enhancement of a U-Slot patch antenna using dual-band frequency selective surface with double rectangular ring elements," *Microw. Opt. Technol. Lett.*, vol. 53, no. 7, pp. 1547-1553, July 2011.

[14] H. Y. Chen and Y. Tao, "Performance improvement of a U-slot patch antenna using a dual-band frequency selective surface with modified Jerusalem cross elements," *IEEE Trans. Antennas Propagat.*, vol. 59, no. 9, pp. 3482-3486, Sep. 2011.

[15] R. Ulrich, "Far-infrared properties of metallic mesh and its complementary structure," *Infrared Phys.*, vol. 7, no. 1, pp. 37-50, 1967.

[16] M. Philippakis, C. Martel, D. Kemp, M. C. S. M. R. Allan, S. Appleton, W. Damerell, C. Burton, and E. A. Parker, "Application of FSS structures to selectively control the propagation of signals into and out of buildings," ERA Technology, Leatherhead, Surrey, U.K., Tech. Rep., 2004.

[17] M. Gustafsson, A. Karlsson, A. P. P. Rebelo, and B. Widenberg, "Design of frequency selective windows for improved indoor outdoor communication," *IEEE Trans. Antennas Propagat.*, vol. 54, no. 6, pp. 1897-1900, June 2006.

[18] G. I. Kiani, L. G. Osslon, A. Karlsson, and K. P. Esselle, "Transmission of infrared and visible wavelengths through energy-saving glass due to etching of frequency-selective surfaces," *IET Microw. Antennas Propagat.*, vol. 4, pp. 955-961, 2010.

[19] G. I. Kiani, L. G. Osslon, A. Karlsson, K. P. Esselle, and M. Nilsson, "Cross-dipole bandpass frequency selective surface for energy-saving glass used in building," *IEEE Trans. Antennas Propagat*., vol. 59, no. 2, pp. 520-525, Feb. 2011.

[20] D. J. Kern, D. H. Werner, A. Monorchio, L. Lanuzza, and M. J. Wilhelm, "The design synthesis of multiband artificial magnetic conductors using high impedance frequency selective surfaces," *IEEE Trans. Antennas Propagat.*, vol. 53, no. 1, pp. 8-17, Jan. 2005.

[21] J. McVay, N. Engheta, and A. Hoorfar, "High impedance metamaterial surfaces using Hilbert-curve inclusions," *IEEE Microw. Wireless Compon. Lett.*, vol. 14, pp. 130-132, 2004.

[22] J. Bell and M. Iskander, "A low-profile archimedean spiral antenna using an EBG ground plane," *IEEE Antennas Wireless Propagat. Lett*., vol. 3, pp. 223-226, 2004.

[23] F. Costa, S. Genovesi, and A. Monorchio, "On the bandwidth of high-impedence frequency selective surfaces," *IEEE Antennas Wireless Propagat. Lett*., vol. 8, pp. 1341-1344, 2009.

[24] R. Mittra, C. H Chan, and T. Cwik, "Techniques for analyzing frequency selective surfaces - A review," *Pro. IEEE*, vol. 76, no. 12, pp. 1593-1615, Dec. 1988.

[25] B. A. Munk, *Frequency Selective Surfaces - Theory and Design*. John Wiley & Sons, Inc., New York, 2000.

[26] R. Dickie, R. Cahill, H. Gamble, V. Fusco, M. Henry, M. Oldfield, P. Huggard, P. Howard, N. Grant, Y. Munro, and P. de Maagt, "Submillimeter wave frequency selective surface with polarization independent spectral responses," *IEEE Trans. Antennas Propagat.*, vol. 57, no. 7, pp. 1985-1994, July 2009.

[27] F. R. Yang, K. P. Ma, Y. Qian, and T. Itoh, "A uniplanar compact photonic-bandgap (UC-PBG) structure and its applications for microwave circuits," *IEEE Trans. Microw. Theory Tech.*, vol. 47, no. 8, pp. 1509-1514, Aug. 1999.

[28] C. N. Chiu, C. H. Kuo, and M. S. Lin, "Bandpass shielding enclosure design using multipole-slot arrays for modern portable digital devices," *IEEE Trans. Electromagn. Compat.*, vol. 50, no. 4, pp. 895-904, Nov. 2008.

[29] M. S. Zhang, Y. S. Li, C. Jia, and L. P. Li, "Signal integrity analysis of the traces in electromagnetic-bandgap structure in high-speed printed circuit boards and packages," *IEEE Trans. Microw. Theory Tech.*, vol. 55, no. 5, pp. 1054-1062, Nov. 2007.

[30] K. Sarabandi and N. Behdad, "A frequency selective surface with miniaturized elements," *IEEE Trans. Antennas Propagat*., vol. 55, no. 5, pp. 1239-1245, May 2007.

[31] T. Kamgaing and O. M. Ramahi, "Design and modeling of high-impedance electromagnetic surfaces for switching noise suppression in power planes," *IEEE Trans. Electromagn. Compat.*, vol. 47, no. 3, pp. 479-489, Aug. 2005.

[32] T. K. Wu and S. W. Lee, "Multiband frequency selective surface with multiring patch elements," *IEEE Trans. Antennas Propagat.*, vol. 42, no. 11, pp. 1484-1490, Nov. 1994.

[33] T. K. Wu, "Four-band frequency selective surface with double-square-loop patch elements," *IEEE Trans. Antennas Propagat.*, vol. 42, no. 12, pp. 1659-1663, Dec. 1994.

[34] H. L. Liu, K. L. Ford, and R. J. Langley, "Design methodology for a miniaturized frequency selective surface using lumped reactive components," *IEEE Trans. Antennas Propagat*., vol. 57, no. 9, pp.

2732-2738, Sep. 2009.
[35] R. R. Xu, H. C. Zhao, Z. Y. Zong, and W. Wu, "Dual-Band capacitive loaded frequency selective surfaces with close band spacing," *IEEE Microw. Wireless Compon. Lett.*, vol. 18, no. 12, Dec. 2008.
[36] G. I. Kiani, K. L. Ford, K. P. Esselle, A. R. Weily, C. Panagamuwa, and J. C. Batchelor, "Single-layer bandpass active frequency selective surface," *Microw. Opt. Technol. Lett.*, vol. 50, no. 8, pp. 2149-2151 Aug. 2008.
[37] G. I. Kiani, K. L. Ford, K. P. Esselle, A. R. Weily, and C. J. Panagamuwa, "Oblique incidence performance of a novel frequency selective surface absorber," *IEEE Trans. Antennas Propagat.*, vol. 55, no. 10, pp. 2931-2934, Oct. 2007.
[38] B. A. Munk, P. Munk, and J. Pryor, "On designing Jaumann and circuit analog absorbers (CA absorbers) for oblique angle of incidence," *IEEE Trans. Antennas Propagat.*, vol. 55, no. 1, pp. 186-193, Jan. 2007.
[39] A. K. Zadeh and A. Karlsson, "Capacitive circuit method for fast and efficient design of wideband radar absorbers," *IEEE Trans. Antennas Propagat.*, vol. 57, no. 8, pp. 2307-2314, Aug. 2009.
[40] A. Itou, O. Hashimoto, H. Yokokawa, and K. Sumi, "A fundamental study of a thin wave absorber using FSS technology," *Electron. Commun. Jpn.*, vol. 87, pt. 1, pp. 77-86, 2004.
[41] A. Itou, H. Ebara, H. Nakajima, K. Wada, and O. Hashimoto, "An experimental study of a wave absorber using a frequency-selective surface," *Microw. Opt. Technol. Lett.*, vol. 28, pp. 321-323, 2001.
[42] G. I. Kiani, A. R. Weily, and K. P. Esselle, "A novel absorb/transmit FSS for secure indoor wireless networks with reduced multipath fading," *IEEE Microw. Wireless Compon. Lett.*, vol. 16, no. 6, pp. 378-380,2006.
[43] N. Engheta and R. W. Ziolkowski, *Metamaterials: Physics and Engineering Explorations*. Hoboken/ Piscataway, NJ: Wiley-IEEE Press, 2006.
[44] R. Baggen, M. Martinez-Vazquez, J. Leiss, and S. Holzwarth, "Comparison of EBG substrates with and without vias for GALILEO/GPS applications," In *Proc. EuCAP 2007, 2nd European Conf. Antennas Propagat.*, Edinburgh, UK, 2007.
[45] Y. Fan, B. L. Ooi, H. D. Hriston, and M. S. Leong, "Compound diffractive lens consisting of Fresnel zone plate and frequency selective screen," *IEEE Trans. Antennas Propagat.*, vol. 58, no. 6, pp. 1842-1847, June 2010.
[46] P. Harms, R. Mittra, and W. Ko, "Implementation of the periodic boundary-condition in the finite-difference time-domain algorithm for FSS structures," *IEEE Trans. Antennas Propagat.*, vol. 42, no. 9, pp. 1317-1324, Sep. 1994.
[47] J. L. Volakis, T. Ozdemir, and J. Gong, "Hybrid finite-element methodologies for antennas and scattering," *IEEE Trans. Antennas Propagat.*, vol. 45, no. 3, pp. 493-507, Mar. 1997.
[48] T. W. Leonard and J. W. Cofer, "A new equivalent circuit representation for the Jerusalem cross," in *Proc. IEE Int. Conf. Antennas Propagat.*, London, England, vol. 2, pp. 65-69, 1978.
[49] R. J. Langley and A. J. Drinkwater, "Improved empirical model for the Jersalem cross," *IEE Proc.*, vol. 129, Pt. H., no.1, pp. 1-6, Feb. 1982.
[50] M. Hosseinipanah and Q Wu, "Equivalent circuit model for designing of Jerusalem cross-based artificial magnetic conductors," *Radioeng*., vol. 18, no. 4, pp. 544-550, Dec. 2009.
[51] T. Cwik, R. Mittra, K. Lang, and T. K. Wu, "Frequency selective screens," *IEEE Antennas Propagat. Soc. Newslett.*, vol. 29, no. 2, pp. 5-10, Apr. 1987.
[52] T. K. Wu, "Dielectric properties measurement of substrate and support materials," *Microw. Opt. Technol. Lett.*, vol. 3, no. 8, pp. 283-286, Aug. 1990.
[53] L. B. Wang, K. Y. See, J. W. Zhang, B. Salam, and A. C. W. Lu, "Ultrathin and flexible screen-printed metasurfaces for EMI shielding application," *IEEE Trans. Electromagn. Compat.*, vol. 53, no. 3, pp. 700-705, Aug. 2011.
[54] L. H. Lafara, *Computer Method for Science and Engineering*. New York: Hayden, 1973, pp. 148-157.
[55] H. Y. Chen, T. H. Lin, and P. K. Li, "Fast design of Jerusalem-cross parameters by equivalent circuit model and least-square curve fitting technique," *Appl. Comput. Electromagn. Soc. J.*, vol. 30, no. 7, pp. 717-730, July 2015.

Hsing-Yi Chen was born in Taiwan, in 1954. He received the B.S. and M.S. degrees in Electrical Engineering in 1978 and 1981 from Chung Yuan Christian University and National Tsing Hua University, respectively. He received the Ph.D. degree in Electrical Engineering from University of Utah, Salt Lake City, Utah in 1989. He joined the faculty of the Department of Electrical Engineering, Yuan Ze University, Taiwan, in September 1989. He was the Chairman of Electrical Engineering from 1996 to 2002, the Chairman of Communications Engineering from 2001 to 2002, the Dean of Engineering College from 2002 to 2006, the Dean of Electrical and Communication Engineering College from 2006 to 2012, and the Dean of Research and Development Office from

2012 to 2013. Currently, he is the Dean of General Affairs Office, Yuan Ze University. His current interests include electrostatic discharge, electromagnetic scattering and absorption, waveguide design, radar systems, electromagnetic compatibility and interference, bioelectromagnetics, electromagnetic radiation hazard protection, and applications of frequency selective surface.

He is a member of Phi Tau Phi. He was also a member of the editorial board of the *Journal of Occupational Safety and Health* from 1996 to 1997. He was elected an Outstanding Alumnus of the Tainan Second High School in 1995. He has been the recipient of numerous awards including the 1990 Distinguished Research, Service, and Teaching Award presented by the Yuan Ze University, the 1999 and 2002 YZU Outstanding Research Award, and the 2005 Y. Z. Hsu Outstanding Professor Award for Science, Technology & Humanity Category. He was awarded Chair Professor by Far Eastern Y. Z. Hsu Science and Technology Memorial Foundation in 2008. His name is listed in Who's Who in the World in 1998.

Shu-Huan Wen was born in Taiwan, in 1991. He received the B.S. degree in Electronic Engineering from Oriental Institute of Technology in 2013. He is currently working toward the Ph.D. degree in Communications Engineering at Yuan Ze University, Taiwan. His research interests include patch antenna design, frequency selective surfaces, EM field measurement, and computational electromagnetics.